

YEON-WOOK KIM<sup>1\*</sup>, BAGUS D. ERLANGGA<sup>1</sup>, DALHYUN DO<sup>1</sup>, SEONG-MIN LEE<sup>2</sup>

**EFFECT OF CONTROLLED POROSITY ON THE MECHANICAL PROPERTIES  
OF Ti-Zr-Sn-Mo BIOMEDICAL ALLOYS**

In this study, a simple and effective way to fabricate highly porous scaffolds with controlled porosity and pore size is demonstrated. Ti-7Zr-6Sn-3Mo shape memory alloy fibers were prepared through a melt overflow process. The scaffolds with porosity of 65-85% and large pores of 100-700 µm in size were fabricated by sintering the as-solidified fibers. Microstructures and transformation behaviors of the porous scaffolds were investigated by means of SEM, DSC and XRD. The scaffolds were composed of  $\beta$  phase at room temperature. Superelasticity with the superelastic recovery strain of 7.4% was achieved by  $\beta \leftrightarrow \alpha''$  phase transformation. An effect of porosity on mechanical properties of porous scaffolds was investigated by using compressive test. As the porosity increased from 65% to 85%, elastic modulus and compressive strength decreased from 0.95 to 0.06 GPa and from 27 to 2 MPa, respectively.

*Keywords:* Ti-Zr-Sn-Mo alloy, Porous scaffolds, Biomedical materials, Shape memory alloys

## 1. Introduction

Osteoporosis is one of the serious diseases for aged people around the world. This leads to reduce the dense of trabecular or cancellous bones which is having relatively high porosity. It is estimated that 50% women and 20% men over their 50 years of age experience an osteoporosis in some part of the bones [1]. Bone replacement surgery is a straightforward alternative to cope with osteoporosis. The replacing materials have to meet the requirement of mechanical properties of the corresponding bone tissue as well as their biocompatibility. TiNi shape memory alloys have already been extensively applied as metallic biomaterials in making biomedical apparatus and implant devices, such as orthodontic arch wires and bone plates, due to their good biocompatibility, excellent corrosion resistance and low elastic modulus [2]. However, there have been a concern regarding the risk of Ni allergy and hypersensitivity for long term use [3]. Recently,  $\beta$ -Ti shape memory alloys have an attracted attention due to their good biocompatibility and Ni-free biomaterials. Endoh et al. have reported that Ti-Zr-Mo-Sn alloys exhibit superelasticity at body temperature for use as biomedical materials [4]. Furthermore, Ni-free Ti-based shape memory alloys in porous form have attracted an additional interest as biomaterials

for implantation since the introduction of pores into the bulk material provides ingrowth of living tissues and firm fixation in addition to producing light weight ductile shape memory alloys [5,6]. Especially, it is possible to decrease the elastic modulus of the implants by increasing their porosity. The increased porosity reduces the mismatch in stiffness between bone and implant and then eliminates stress shielding effects which shorten the lifetime of the implant through bone resorption and loosening [7].

Powder metallurgy is known to be a promising method for the production of porous near-net-shape components [8]. It was reported that the porosity produced by self-propagating high temperature synthesis (SHS) of elemental Ti and Ni powders as well as by powder metallurgical process of Ti-Ni alloy powders was less than 60% [9]. However, porosity levels would need to be relatively higher, in order to bring down the stiffness of the metallic materials sufficiently to match that of bone. Such high porosity would also favor bone in-growth, and hence good adhesion. In this study, a new method to fabricate the highly porous shape memory alloys is proposed. Fine Ti-7Zr-6Sn-3Mo (at%) alloy fibers were prepared through a melt overflow process. The porous scaffolds were produced by using the solid-state sintering of the fibers, and the effect of the high porosity on the mechanical performances was investigated.

<sup>1</sup> KEIMYUNG UNIVERSITY, DEPARTMENT OF ADVANCED MATERIALS ENGINEERING, 1000 SHINDANG-DONG DALSEO-GU, DAEGU 704-701, KOREA

<sup>2</sup> UNIVERSITY OF INCHEON, INCHEON, REPUBLIC OF KOREA

\* Corresponding author: ywk@kmu.ac.kr



## 2. Experimental

Ti-7Zr-6Sn-3Mo (at%) alloy ingots were prepared from high purity elements of titanium, nickel and molybdenum by a non-consumable arc-melting system under an argon atmosphere. The ingots were re-melted more than five times under a high purity of argon atmosphere to achieve the homogeneous chemical composition. In the present study, the experimental works to make fine alloy fibers were performed by using a laboratory scale arc melt overflow. About 30 grams of the ingot was placed in a water-cooled hearth, and skull-melted under argon atmosphere by a plasma beam. Then, the hearth was tilted about the rotating quenching wheel, which was made of molybdenum. The liquid metal overflowed over a relatively horizontal edge or pour spot, to contact the cooling wheel surface. The quenching wheel substrate served as a continuous permanent mold, against which the casting solidified. The thickness of the fibers can be controlled by the rotating speed of the wheel. The dimension of the Mo cooling wheels was 122 mm and 10 mm in diameter and width. Its tip was acutely machined, in order to produce the shape of fibers or filaments. The speed of the cooling wheel was kept at 1200 rpm to produce relatively thin fibers.

These rapidly solidified fibers were cut into segments with the length ranged from 5 to 10 mm. The fiber segments were uniformly put into the predetermined packing chamber of the graphite mold and then pressure was applied by screwing the bolts so as to conform the strong contact of fibers during sintering. Sintering was carried out in a vacuum induction furnace under a high vacuum atmosphere. The sintering temperature and time were 1300°C and 30 min, respectively. Fractional porosity is defined as the ratio of pore volume to total volume [10]. The scaffolds with three different porosities were fabricated to investigate the effect of porosity on mechanical properties. It was reported that the porosity of the scaffold was about 70-90% in cancellous bone [11]. Thus, in this study, the scaffolds of 65, 75 and 85% porosity were fabricated by filling the cavity of the designed mold with 2.8217, 2.0155 and 1.2093 grams of the fibers, respectively. Transformation temperatures were measured by using differential scanning calorimetry (DSC) at a cooling and heating rate of 10 °C /min. Crystal phases were identified by using X-ray diffraction (XRD), with CuK $\alpha$  radiation. Microstructural investigations were performed by FE-SEM (ZEISS GeminiSEM 300). The mechanical properties of the porous scaffolds were investigated by uniaxial compression experiments (an Instron 6820 model) with a strain rate of 0.24 mm/min.

## 3. Results and Discussion

Fig. 1 shows the rapidly solidified Ti-7Zr-6Sn-3Mo alloy fibers prepared by the melt overflow processing. The continuous fibers of about 70  $\mu$ m diameter were fabricated at the linear speed of 7.7 m/s under a high vacuum atmosphere. DSC measurement was performed to investigate the transformation behavior of the fibers. Fig. 2(a) shows the DSC curve of the as-solidified fibers.

Any DSC peak was observed during heating and subsequent cooling. This may be due to the small enthalpy of the transformation associated with  $\beta$  (parent phase)  $\rightarrow$   $\alpha''$  (martensitic phase) [12]. Fig. 2(b) shows XRD profile of the as-solidified fiber at



Fig. 1. A photograph of as-solidified Ti-7Zr-6Sn-3Mo (at%) fibers fabricated by a melt overflow process

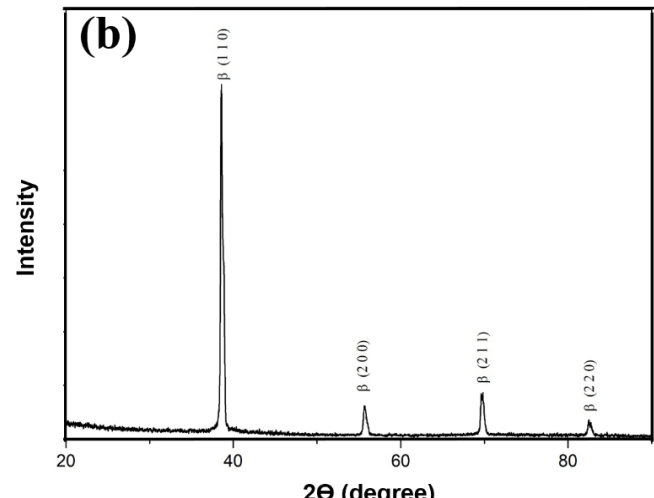
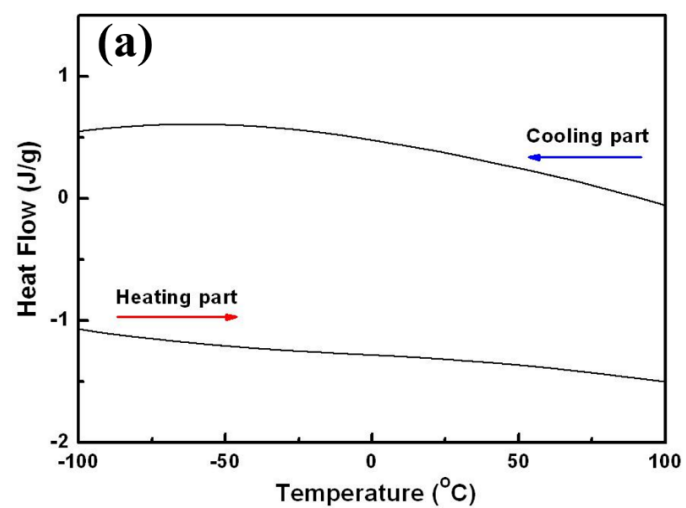


Fig. 2. (a) DSC curve and (B) XRD pattern of as-solidified Ti-7Zr-6Sn-3Mo fibers

room temperature (298 K). The fibers appeared to be single  $\beta$  phase with four XRD peaks of  $\beta(110)$ ,  $\beta(200)$ ,  $\beta(211)$  and  $\beta(220)$ . This result reflects that the  $\beta \rightarrow \alpha''$  martensitic transformation and the  $\alpha'' \rightarrow \beta$  reverse martensitic transformation do not occur at room temperature, and then  $M_s$  (martensitic transformation start temperature) and  $A_f$  (reverse martensitic transformation finish temperature) of the fibers are lower than room temperature.

The as-solidified fibers were sintered under a low press to make the firm bond that linked one fiber to another, and then large pores were formed. Fig. 3(a) shows the photograph of the scaffolds with three different porosities of 65%, 75% and 85%, respectively. The dimension of the as-sintered scaffolds was 10 mm width, 10 mm length and 15 mm height. SEM images were taken from the cross-section of the as-sintered scaffolds.

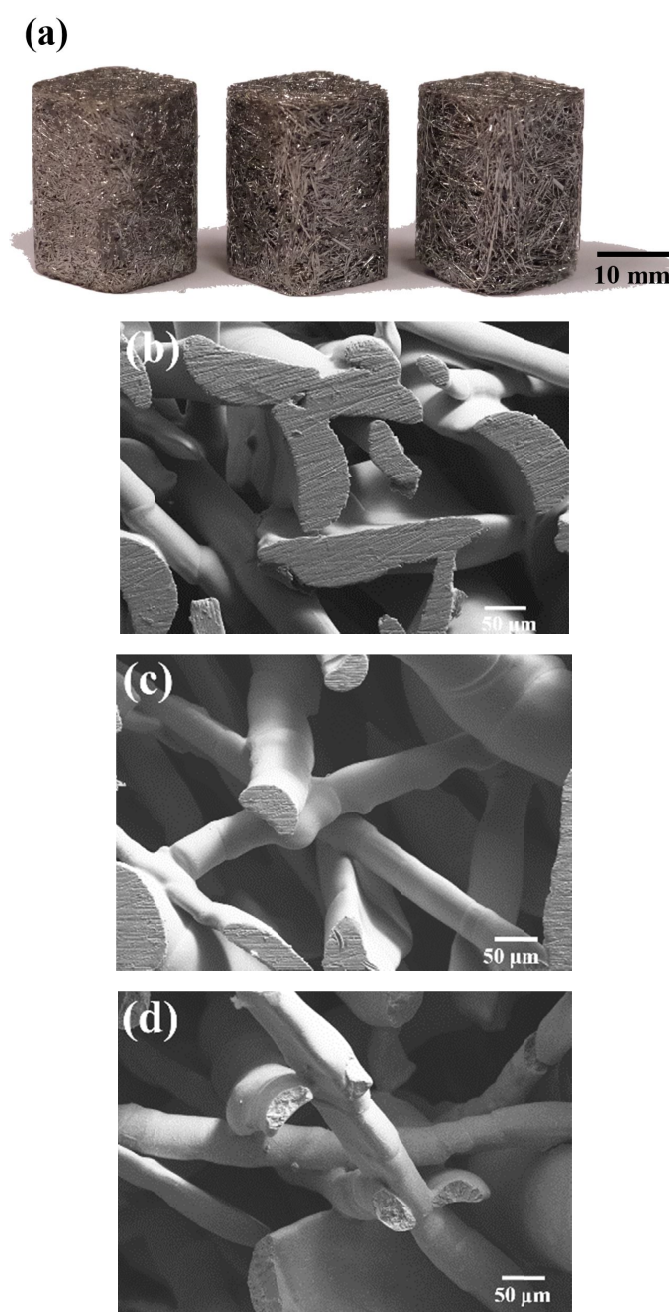


Fig. 3. (a) A photograph of as-sintered Ti-7Zr-6Sn-3Mo scaffolds and SEM images of the scaffolds with (b) 65, (c) 75, and (d) 85% porosity

Fig. 3 (b)–(d) show SEM micrographs of the scaffolds with 60, 70 and 80% porosity, respectively. Most sintering joints were produced between two single fibers at crossover points during sintering. The pores, which were formed by three-dimensionally networking structures of the thin fibers, were fully interconnected as open-cell geometries. The pore size of the scaffolds varied widely from 100 to 700 μm. However, the average pore size could be controlled by a variation of the porosity, and then the increase of porosity resulted in a substantial increase of the pore size, as shown in Fig 3(b)–(d). It is well known that the larger pore size is good for enhancing bone ingrowth. Itin *et al.* reported that the size of pores in porous bone substitutes varying from 100 to 500 μm was optimal for new bone tissue ingrowth [13]. In this study, the porous scaffolds fabricated by the fibers matches well with the requirement of porosity and pore size in cancellous bone. Therefore, the open-pores in the Ti-Zr-Sn-Mo alloy scaffold are large enough to provide space for ingrowing tissue cells and extensive body fluid transportation through the scaffold matrix.

Loading-unloading compressive tests were carried out to investigate the mechanical behaviors of porous Ti-Zr-Sn-Mo shape memory alloy scaffolds. The compressive stress was applied until the deformation strain reached 15%, after which it was released at the same ramp rate, as shown in Fig. 4. The stress-strain curves showed two stages of deformation: a linear region corresponding to initial stage of elastic deformation of the parent  $\beta$  phase, and a stress plateau region corresponding to stress-induced martensitic transformation stage. The stress for martensitic transformation of the scaffolds decreased rapidly from 15 MPa to 1.5 MPa, when the porosity increased from 65 to 85%. The increase of the porosity from 65 to 85% resulted in a rapid decrease of the compressive strength from 27 to 2 MPa at 15% strain. After unloading, superelastic behaviors were observed in all scaffolds. The elastic recovery strain ( $\epsilon_{el}$ ) and the superelastic recovery strain ( $\epsilon_{se}$ ) were indicated in Fig. 4. The superelastic recovery increased with increase in the porosity, and the maximum superelastic recovery of 7.4 % was observed in the scaffold of 85% porosity.

In Fig. 4, variation of the elastic moduli obtained from the stress-strain curves is shown as the function of the porosity. Upon increasing the porosity from 65 to 85%, the elastic modulus decreased from 0.95 to 0.06 GPa. Their low elastic moduli are the valuable mechanical property of porous Ti-7Zr-6Sn-3Mo scaffolds. Elastic modulus of cancellous bone is between 0.1 and 2 GPa and its compressive strength is between 2 and 20 MPa [14]. Even though TiNi alloys have similar deformation behavior with that of bone compared with other metallic materials [15], the elastic moduli of fully dense TiNi alloys range from 40 to 90 GPa for austenite phase and from 20 to 50 GPa for martensite phase [16,17], which are still higher than that of cancellous bone. However, the mechanical properties (compressive strength, superelastic strain and modulus) of the porous Ti-Zr-Sn-Mo scaffolds meet the requirements of mechanical properties for cancellous bone, and then the porous Ti-Zr-Sn-Mo scaffolds must be a great potential implant material to replace the damaged cancellous bone.

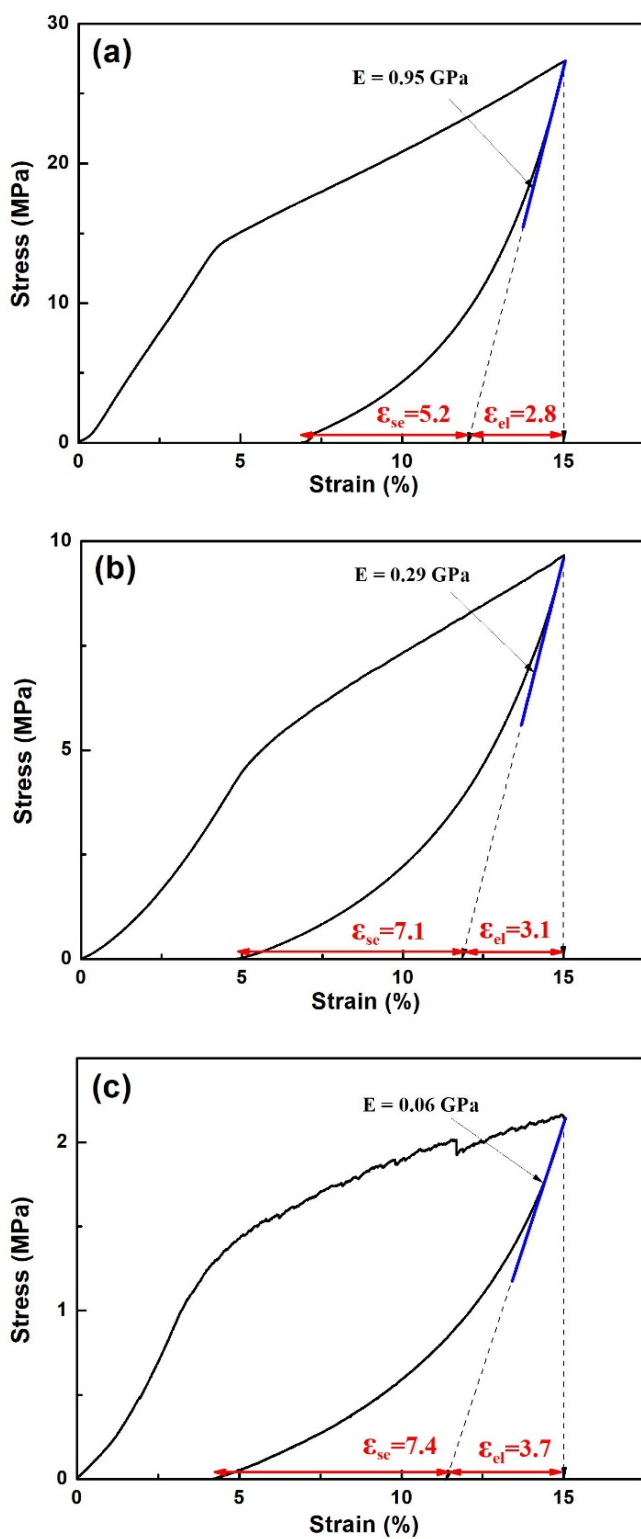


Fig. 4. Compressive stress-strain curves of the scaffolds with (a) 65, (b) 75 and (c) 85% porosity

#### 4. Conclusions

Ti-Zr-Sn-Mo shape memory alloy fibers were prepared through a melt overflow process. Ni-free scaffolds with a range of porosity from 65 to 85 % were synthesized by the solid-state sintering of as-solidified fibers. The pores exhibited three-

dimensionally networking structures of the thin fibers and were fully interconnected as open-cell. The pore size varied widely from 100 to 700  $\mu\text{m}$ . These open-pores were large enough to transport extensive body fluid and facilitated bone ingrowth. The porous scaffold exhibited the excellent superelasticity with a recovery strain of 7.4% at room temperature. Upon increasing the porosity of scaffolds from 65 to 85%, the elastic modulus and the compressive strength decreased from 0.95 to 0.06 GPa and from 28 to 2 MPa, respectively. These excellent mechanical properties for implant materials matched well with those of cancellous bone, which could reduce the stress shield effect.

#### Acknowledgements

This research was supported by Basic Science Research Program through the National Research Foundation of Korea (NRF) funded by the Ministry of Education, Science and Technology (2017R1A2B4005693)

#### REFERENCES

- [1] T. Sozen, L. Ozisik, N.C. Basaran, European Journal of Rheumatology **4**, 1, 46 (2016).
- [2] J.I. Helsen, H.J. Breme, Metals as Biomaterials, 1st ed., John Wiley & Sons, United Kingdom (1998).
- [3] A. Biesiekierski, J. Wang, M. Abdel-Hady Gepreel, and C. Wen, Acta Biomaterialia **8**, 5, 1661 (2012).
- [4] K. Endoh, M. Tahara, T. Inamura, and H. Hosoda, Materials Science and Engineering A **704**, 72 (2017).
- [5] J.Y. Xiong, Y.C. Li, X.J. Wang, P.D. Hodgson, C.E. Wen, J. Mech. Behav. Biomed. Mater. **1**, 269 (2008).
- [6] C. Greiner, S.M. Oppenheimer, D.C. Dunand, Acta Biomater. **1**, 705 (2005).
- [7] G. Ryan, A. Pandit, B. Apatsidis, Biomaterials **27**, 2651 (2006).
- [8] M. Köhl, T. Habijan, M. Bram, H.P. Buchkremer, D. Stöver, and M. Köller, Advanced Engineering Materials **11**, 12, 959 (2009).
- [9] G. Qiu, J. Wang, H. Cui, and T. Lu, SN Applied Sciences **1**, 1, 56 (2018).
- [10] S. Wu, C.Y. Chung, X. Liu, P.K. Chu, K. J.P.Y. Ho, C.L. Chu, Y.L. Chan, K.W.K. Yeung, W.W. Lu, K.M.C. Cheung, K.D.K. Luk, Acta Mater. **55**, 3437 (2007).
- [11] Z. H. Wang, C.Y. Wang, C. Li, Y.G. Qin, L. Zhong, B.P. Chen, Z.Y. Li, H. Liu, F. Chang, J.C. Wang, J. Alloy. Comp. **717**, 271 (2017).
- [12] J.I. Kim, H.Y. Kim, T. Inamura, H. Hosoda, S. Miyazaki, Mater. Sci. Eng. A **403**, 334 (2005).
- [13] V.I. Itin, V.E. Gyunter, S.A. Shabalovskaya, R.L.C. Sachdeva, Mater. Char. **32**, 179 (1994).
- [14] S. Bose, M. Roy, A. Bandyopadhyay, Trends Biotechnol. **30**, 546 (2012).
- [15] S.A. Shabalovskaya, Mater. Eng. **12**, 69 (2002).
- [16] Y.W. Kim, Intermetallics **62**, 56 (2015).
- [17] Y.F. Zheng, B.B. Zhang, B.L. Wang, L. Li, Q.B. Yang, L.S. Cui, Acta Biomater. **7**, 2758 (2011).